Bulletin of the Seismological Society of America, Vol. 96, No. 6, pp. 2441–2448 December 2006, doi: 10.1785/0120060038

Short Note

Frequency-Dependent Crustal Correction for Finite-Frequency Seismic Tomography

by Ting Yang* and Yang Shen

Abstract Removing the crustal signature from teleseismic travel times is an important procedure to reduce the trade-off between crustal and mantle velocity heterogeneities in seismic tomography. Because reverberations of long- and short-period body-wave arrivals in the crust affect the waveforms of the direct arrivals differently, the crustal effects on travel times measured by waveform cross correlation are frequency dependent. With synthetic responses of selected crustal models, this short note illustrates the significance of frequency-dependent crustal corrections to finite-frequency body-wave travel-time tomography. The differences in crustal correction between long- and short-period body waves at the same station can be as large as 0.6 sec, depending on the crustal thickness, velocity contrast at the Moho, and layering within the crust.

Introduction

Variations in station elevation and crustal structure beneath seismic stations are responsible for a significant fraction of observed teleseismic body-wave travel-time anomalies. In regions having large variations in crustal thickness (e.g., eastern Eurasia and central Andes) or complex crustal structure, the crust may account for half of the observed travel-time residuals (Kissling, 1993; Beck *et al.*, 1996; Martin *et al.*, 2005). In teleseismic body-wave tomographic studies, the crustal and shallow-mantle structure usually cannot be directly resolved in the inversion because incident waves from teleseismic events propagate nearly vertically and do not cross each other at shallow depths (e.g., Wolfe *et al.*, 1997). If crustal anomalies are not removed from travel-time residuals, they tend to be mapped into deeper mantle, causing artificial velocity anomalies in tomographic models (e.g., Waldhauser *et al.*, 2002). Travel-time correction for shallow structure, therefore, has been an essential procedure in seismic tomography to improve the resolution in the mantle.

There are two common approaches to cope with this problem. The first is to add an additional unknown for each station to be solved in the inversion (e.g., Evans and Achauer, 1993; VanDecar *et al.*, 1995; Wolfe *et al.*, 1997; Foulger *et al.*, 2001). These additional unknowns, or station terms, are used to account for travel-time anomalies associated with the crustal and shallow-mantle structure and are solved simultaneously with the velocity structure in the inversion. One notable characteristic of this approach is that the station terms include the effects from both the crust and shallow mantle. Thus for studies with a large station spacing, the shallow-mantle structure is usually "absorbed" into the station terms and unresolved. By definition, the station terms do not vary with frequencies, epicentral distances, and backazimuths of incoming waves.

For regions where the crustal structure has been determined from other observations such as surface-wave studies, receiver function analyses, and/or reflection and refraction seismic profiles, the crustal effects relative to a reference model can be removed by subtracting the travel-time anomalies accrued within the crust from the total travel-time delays. The residual travel-time delays are then used to invert the mantle structure (e.g., Dawson *et al.*, 1990; Allen *et al.*, 2002; Keyser *et al.*, 2002). Compared with the station-term method, this approach is valuable for imaging the shallow-mantle structure (e.g., Allen *et al.*, 2002), in particular, when the *a priori* crustal structure is considered to be well constrained. Crustal corrections in this approach may vary with epicentral distances and backazimuths of incoming waves. They are usually calculated for the direct arrival under ray theory without any consideration to the reverberation of the wave in the crust (e.g., Allen *et al.*, 2002; Waldhauser *et al.*, 2002; Hung *et al.*, 2004; Martin *et al.*, 2005). When the arrival time of a seismic phase is handpicked from the onset of the arrival, ray theory is commonly used and justified by the argument that the onset represents the arrival of the highest-frequency signal in the seismogram. But it is often difficult to pick the onset of the arrival accurately when the

*Present address: Jackson School of Geoscience, the University of Texas at Austin, 1 University Station C1100, Austin, Texas 78712.

arrivals are long period, emergent, or of less-than-excellent signal-to-noise ratio.

The availability of digital seismic records has made it a common practice to obtain travel times by cross-correlating seismic waveforms (VanDecar and Crosson, 1990). For finite-frequency seismic signals, reverberations of the arrival in the crust beneath a station may overlap with the direct arrival and thus may significantly change the waveform of the direct arrival. The travel times obtained by waveform cross-correlation are therefore sensitive to crust reverberations, especially at low frequencies and for the crust with strong reflectors at shallow depth. As a result, the correction calculated for the direct ray path under ray theory cannot fully account for the effects of crustal variations on travel times measured by waveform cross correlation.

This problem is often neglected in ray-based tomography and has now become more severe for the newly developed finite-frequency seismic tomography (FFST), in which the travel-time calculation is based on 3D sensitivity kernels (Dahlen *et al.*, 2000) instead of ray theory. Because the 3D volumes of low-frequency kernels are broader than those of higher-frequency signals, low-frequency signals offer constraints on the structure farther away from geometrical rays. This more realistic representation of wave propagation helps to obtain a smoother, more even sampling of the velocity structure beneath stations. At ocean bottom and ocean island environments, where the microseism is high (Wilcock *et al.*, 1999), most useful arrivals with good signal-to-noise ratios are in the low-noise notch (roughly 0.03–0.1 Hz; Webb, 1998), the low-frequency range in teleseismic body-wave tomography. To isolate the microseism, Hung *et al.* (2004), Shen and Hung (2004), and Yang *et al.* (2006) filtered broadband *P*-wave records in the high-, intermediate-, and low-frequency bands (0.5–2, 0.1–0.5, and 0.03–0.1 Hz, respectively), and combined the travel times measured in the three frequency ranges in joint tomographic inversions. About 60% of the useful *P*-wave arrivals in the Iceland data set, for example, is long period. For these reasons, long-period travel-time data and their correction for crustal effects are important in FFST, which offers the potential to utilize more information in broadband waveforms than ray theory.

Here we present a crustal correction method, in which crustal reverberations for arrivals with different frequencies are taken into account. Using synthetic waveforms, we show that the crustal correction can be approximated by the waveform shift measured by cross correlation of the response of a given crustal model and that of the reference model in a narrow-frequency band.

Effects of Crustal Reverberations on Travel Times

We use synthetic seismograms to demonstrate that the effects of body-wave reverberations in the crust beneath a station on travel times measured by waveform cross correlation are frequency dependent. We construct synthetic seismograms by convolving a source time series with the impulse response of a crustal model. Our source function is chosen to be the first derivative of a Gaussian pulse, of the form

$$src(t) = -8\pi^2 \tau^{-2} \left(t - \frac{1}{2}\tau\right) \exp\left[-4\pi^2 \left(\frac{t}{\tau} - \frac{1}{2}\right)^2\right] \quad (1)$$

where the frequency content of this source function is controlled by τ. This time function is a full-cycle pulse (shown in Fig. 1a). The impulse responses are computed for a given layered crustal model and a ray parameter using Kennett's reflectivity matrix approach (Kennett, 1983). The calculation yields a full response including mode conversions. For our purposes, we consider the response at the free surface.

Figure 1 shows the procedure of calculating synthetic seismograms from two crustal models and the frequency-dependent crustal corrections obtained from waveform cross correlation. One of the models is the IASP91 (Kennett and Engdahl, 1991). The other is the crustal structure beneath the Global Seismic Network (GSN) station DGAR (7.412° S, 72.453° E), an ocean island site with a relatively thin crust, from CRUST2.0 (Bassin *et al.*, 2000). For simplicity, the first four layers in CRUST2.0 (water, ice, and soft and hard sediment) are not included in the calculations. This is reasonable because permanent seismic stations are usually set up on bedrocks. The thickness, V_p, V_s, and density of each layer in the two crustal models are shown in Figure 1b. Figure 1c shows the calculated impulse responses of these two models to an incident *P* wave by the reflectivity matrix method (Kennett, 1983). The impulse responses are then convolved with the source time function (Fig. 1a) to generate synthetic seismograms (Fig. 1d). To find the frequency dependence of the travel-time differences between the two models, we filtered these seismograms using the high-, intermediate-, and low-frequency bands as in Hung *et al.* (2004) (0.5–2, 0.1–0.5, and 0.03–0.1 Hz, respectively). Relative travel-time delays or crustal corrections for the three frequency bands are then measured from the cross correlation of the two filtered seismograms. As shown in Figure 1e, while the travel-time differences are nearly identical for high- and intermediate-frequency signals, the arrival at DGAR at the low frequency is much earlier (by an additional 0.65 sec) than at the intermediate and high frequencies, due to the overlap of crustal reverberations with the long-period direct arrivals and the smaller separation between the reverberations and the direct arrival at the station above a thin crust.

To see how variations in crustal thickness alone affect the travel times measured by waveform cross correlation, we systemically generated crustal models with different crustal thicknesses and repeated the preceding procedure to calculate the corrections relative to the IASP91 model. In this experiment, the crust is a two-layer model, in which the thickness of each layer is increased or decreased by the same

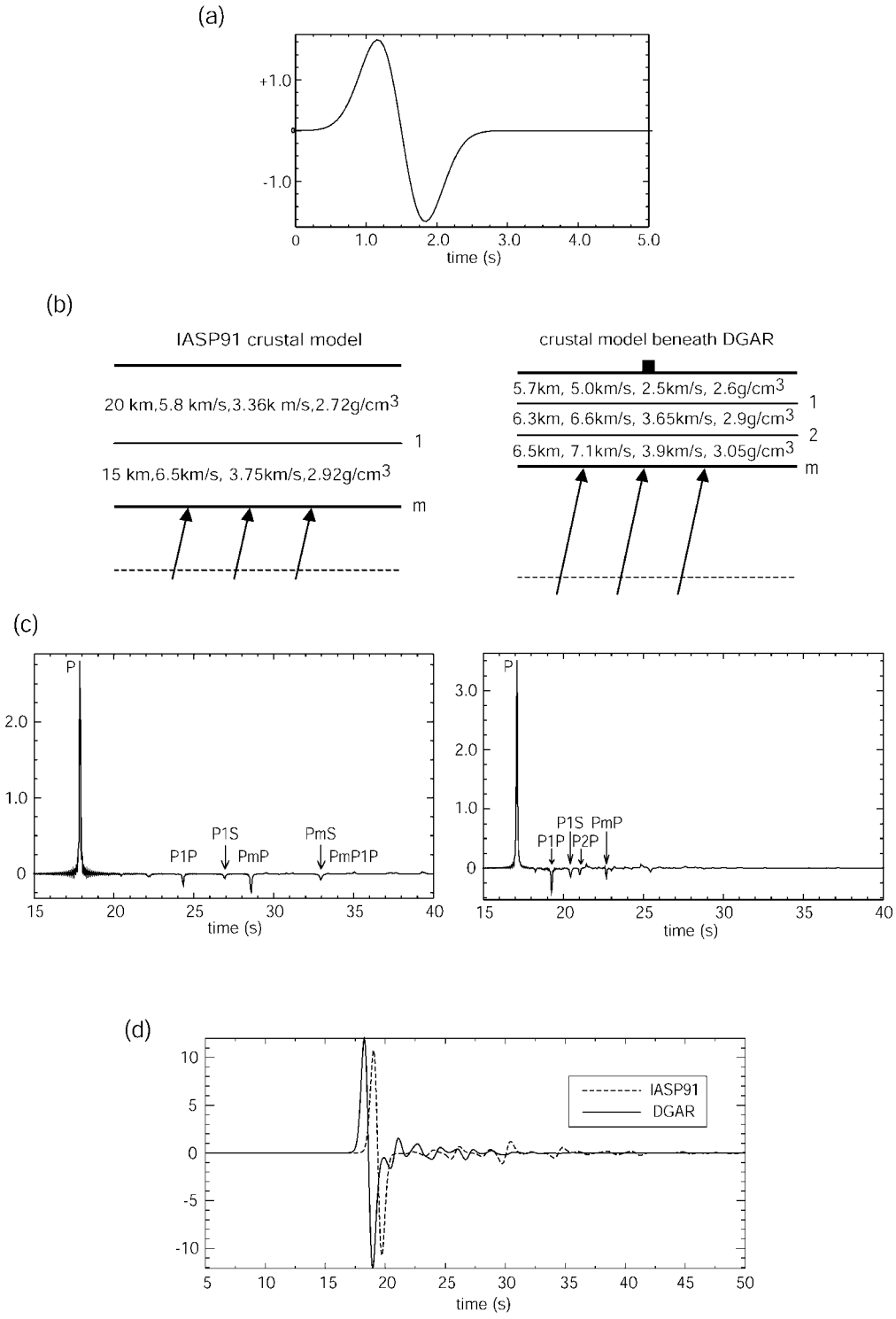

Figure 1. Procedure to generate synthetic seismograms on the vertical component for frequency-dependent crustal correction. (a) Source time function. The power spectrum of this example peaks at about 1 Hz and has energy between 0.001 and 2 Hz. (b) The IASP91 crustal model and a three-layer crustal model beneath the DGAR station from CRUST2.0 (Bassin *et al.*, 2000). Values within layers are thickness, V_p, V_s, and density, respectively. (c) Responses of the IASP91 model and the DGAR crustal model. The major reverberation phases are marked. *PdP* (*PdS*) stands for a *P* wave reflected at the surface and then reflected (converted to *S*) at the discontinuity *d* (1, 2, or the Moho). (d) Synthetic seismograms obtained from the convolution of the source time function and the crustal responses. (e) Bandpass-filtered seismograms for the IASP91 (dashed) and DGAR crust, and travel-time shifts between them measured by cross correlations. (*continued*)

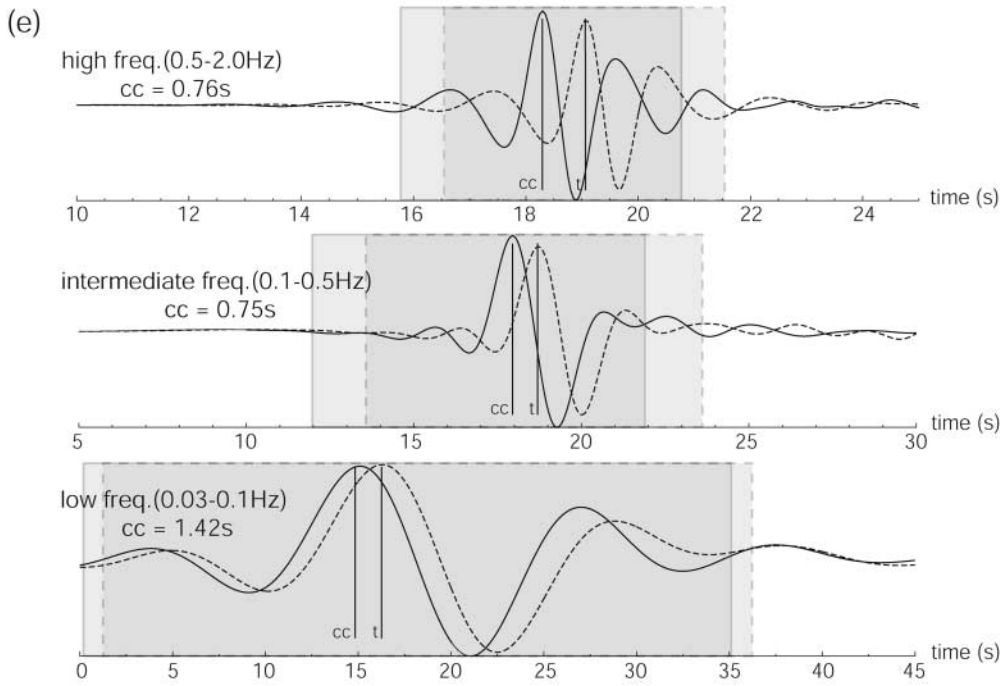

Figure 1. (continued). "*t*" marks the peak of seismograms from the IASP91 model, which is also the cross-correlation reference time; "cc" is the travel-time shift of the two seismograms measured from cross correlation (i.e., crustal correction). Shaded portions with dashed (IASP91) and solid (DGAR) frames indicate the windows for cross correlation. The crustal correction from the ray theory is 0.64 sec, and the ray parameter in this experiment is 0.06 sec/km. The difference between the value predicted by the ray theory and those obtained from waveform crosscorrelation is attributable to the large reverberation from the shallow crust beneath DGAR (*P1P*).

amount incrementally while all other parameters are kept the same as those in IASP91. Figure 2 shows the relationship between the crustal thickness and corrections. Corrections for low-, intermediate-, and high-frequency signals differ when the crustal thickness is less than that of IASP91 (35 km), with the most significant differences in the thickness range of 6–24 km. For the crust with a thickness near or greater than 35 km, the separation between the main reverberation phase (*PmP*) and the direct arrival is greater than 11 sec, sufficiently large that the reverberation does not overlap with the direct arrival and thus does not affect the measured travel times.

To see how internal layering affects the travel time measured by waveform cross correlation, we did a similar experiment with a more complex, three-layer crustal model (Fig. 3). Velocities and densities for this crust model are derived from the average values of the crustal structure beneath 180 eastern Eurasia stations from CRUST2.0 (water, ice, and sediment layers are also excluded), though we arbitrarily fix the thickness of each layer to be one third of the total crustal thickness. These parameters are shown in Table 1. Unlike in Figure 2, the frequency dependence in travel times does not disappear when the crustal thickness is equal to, or larger than that of the reference model (35 km). This is attributable to reverberations in the shallow crust in the three-layer model. So in addition to crustal thickness, the internal layering in the crust, in particular, the strong reflection in the shallow crust, may also have a significant effect on the waveforms and thus the travel times measured by waveform cross correlation.

The preceding synthetic experiments illustrate that, for travel times measured by waveform cross correlation, the effects of crustal reverberations are frequency dependent and must be taken into consideration in tomographic inversions. Crustal corrections calculated simply from ray theory for the direct arrival may leave large biases in the travel times of low-frequency waves and even short-period waves if strong reflectors exist in the shallow (depth <5 km) crust. Since most of the oceanic crust and a significant portion of the continental crust have a thickness within the range of 5 to 30 km, this bias in travel times may significantly degrade the resolution of the mantle structure in seismic tomography (van der Hilst and de Hoop, 2005). Frequency-dependent crustal corrections should be applied in FFST and other studies using low-frequency seismic records.

Practical Considerations

If an accurate crustal structure is available, the effect of crustal reverberations on waveforms can be removed by deconvolving the crustal response from the observed seismograms. The crustal corrections calculated from ray theory

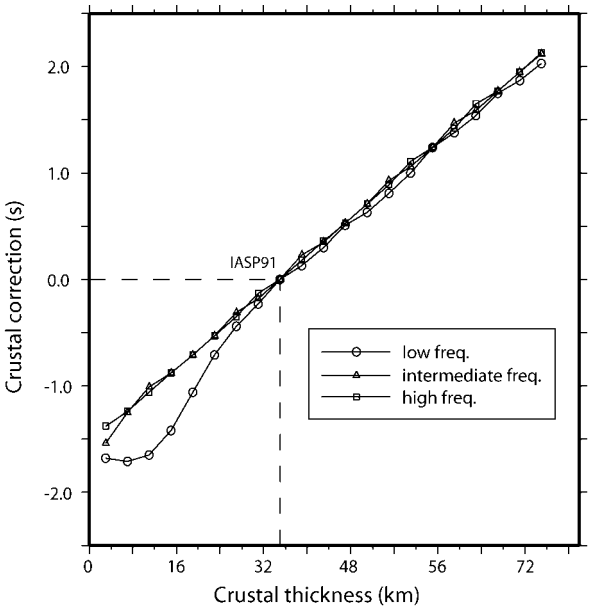

Figure 2. Effect of the crustal thickness on crustal corrections for the high- (0.5–2.0 Hz), intermediate- (0.1–0.5 Hz), and low- (0.03–0.1 Hz) frequency signals. The crust is a two-layer model with the same V_p, V_s, and density as those of IASP91. The thicknesses of the upper and lower crust are increased or decreased by the same amount in each calculation. The source time function is shown in Figure 1a.

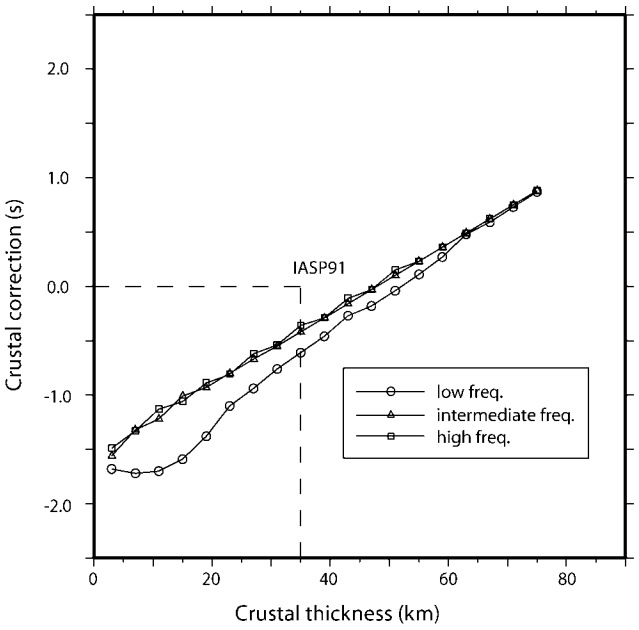

Figure 3. Effects of the crustal thickness and the internal layering on crustal corrections for the high- (0.5–2.0 Hz), intermediate- (0.1–0.5 Hz), and low- (0.03–0.1 Hz) frequency signals. The crust is a three-layer model with V_p, V_s, and density being the mean values of the crust beneath seismic stations in eastern Eurasia from CRUST2.0 (layer 5, 6, and 7) (Bassin *et al.*, 2000). The thickness of each layer is one third of the total crustal thickness. The average *P*-wave crustal velocity (6.55 km/sec) is higher than that in IASP91 (6.08 km/sec). The source time function is shown in Figure 1a.

Table 1
Average Crustal Structure beneath Seismic Stations in Eastern Eurasia* from CRUST2.0

	V_p (km/sec)	V_s (km/sec)	Density (g/cm^3)
Upper crust	5.97	3.39	2.71
Middle crust	6.55	3.67	2.88
Lower crust	7.13	3.95	3.06

*Stations are within the range of (20° S to 60° S, 60° E to 160° E).

can then be used properly for signals at all frequencies. However, this approach may not be practical since the deconvolution process is sensitive to the response, which requires a very accurate crustal model (Obayashi *et al.*, 2004).

Crustal corrections can also be approximated without the deconvolution of recorded waveforms by following the steps in Figure 1. In practice, this may also be achieved by calculating the impulse response of the crustal model directly, and filtering the response within the specified frequency bands. Real seismic records may have a higher energy toward the low-frequency end of the selected frequency band or vice versa. Thus real data may have a spectrum that is somewhat different from the impulse response, whose power spectrum is flat. This mismatch between the spectra of real records and the impulse response may introduce errors into the crustal corrections for travel times measured by waveform cross correlation. Our synthetic experiments show, however, that this error is likely negligible with narrow frequency bands. Figure 4 shows the difference between the correction obtained from synthetic seismograms with a known source time function (cc1) and that directly from the impulse response of the crust (cc2). We conducted this synthetic experiment for two sets of crustal models and several different source time functions having various power spectra. For the three frequency bands and all crustal models with different thicknesses, most of the differences between the two approaches are less than one sampling interval (0.05 sec), and the biggest one is 0.08 sec. This result suggests that, to first order, the crustal corrections within individual frequency bands are not very sensitive to the spectrum of the incoming wave and one may choose to use corrections measured directly from impulse responses to approximate those for observed waveforms.

With the preceding approximations, a first-order crustal correction can be obtained through the following steps:

1. Calculate the ray parameter based on the station and earthquake locations.
2. Calculate the responses of the crustal model beneath the station and the reference model for the ray parameter.

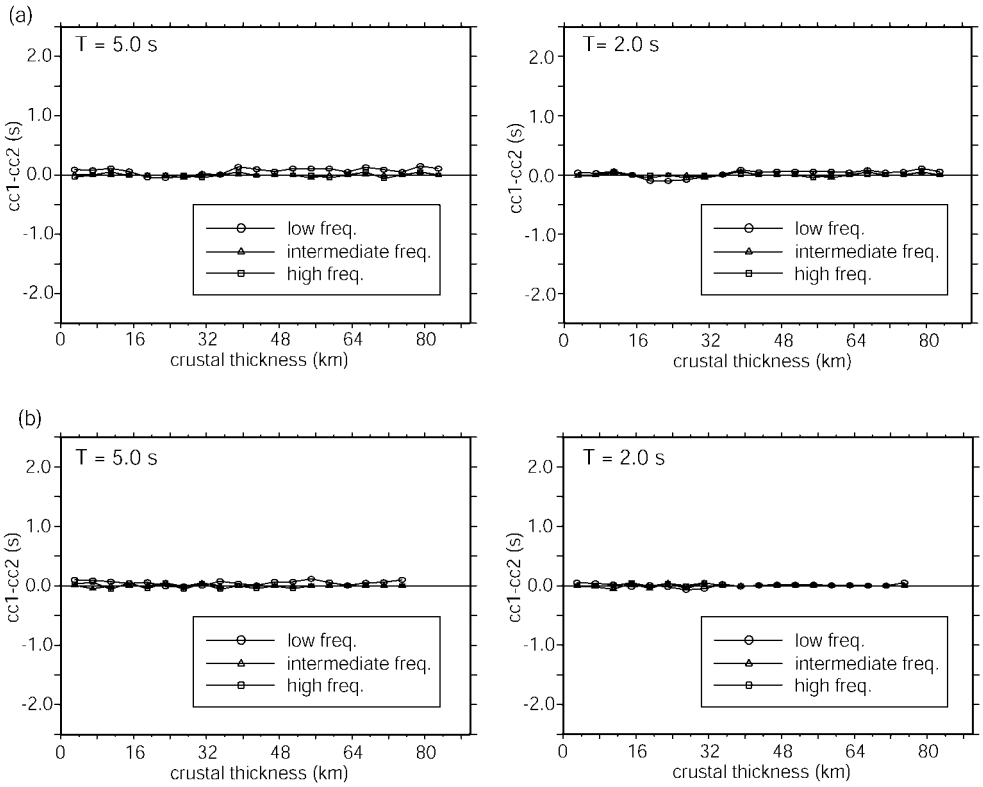

Figure 4. Differences between crustal corrections from synthetic seismograms (cc1) and those from impulse responses (cc2) for the high- (0.5–2.0 Hz), intermediate- (0.1–0.5 Hz), and low- (0.03–0.1 Hz) frequency bands. (a) The two-layer, IASP91-type crust. (b) The three-layer crust, as shown in Table 1. "T" is the apparent period of the source time source (τ) in equation (1).

3. Filter the responses in the same frequency ranges as those of real data.
4. Cross-correlate the two filtered responses from the reference model and the model for a station to measure the correction for a specified frequency band.
5. Apply the correction to the corresponding travel time of the observed waveform at the station.

To get a quantitative estimate of the magnitude of frequency-dependent crustal corrections in a real-world situation, we applied this crust-correction procedure to broadband seismograms recorded at stations in the western Pacific. The crustal models beneath these stations are from CRUST2.0 (Bassin *et al.*, 2000). Figure 5 shows an example of the effect of the frequency-dependent crustal correction on travel time shifts, in which the magnitude of crustal correction is comparable to the relative delays measured by cross correlation and the difference between the high- and low-frequency corrections is as much as 25% of the travel-time delays.

There are two other assumptions in the previous examples that one may consider in the crustal correction. First, the uppermost mantle velocity affects the impedance contrast at the Moho and thus has an effect on the waveform of the crustal reverberation and on the crustal correction. In many cases (e.g., the global crustal model CRUST2.0), the uppermost mantle velocity is unavailable. One has to assume a velocity for the uppermost mantle. To assess how this assumption affects the crustal correction, we changed the uppermost mantle velocity and compared crustal corrections with that based on the IASP91 velocity. A $\pm 3.7\%$ variation in the uppermost mantle velocity (7.75–8.35 km/sec) causes a very small difference (0.035 sec) in the measured low-frequency travel times. Therefore, to first order, the effect of the uppermost mantle velocity is negligible.

Second, we assume flat crustal interfaces in these calculations of the crustal response. The real crust has 2D or 3D variations in velocity and interfaces, which have more complex influences on the waveforms of recorded broadband signals. For regions having well-constrained 2D or 3D crustal models, the crustal responses can be calculated with other techniques (e.g., Komatitsch and Vilotte, 1998; Frederiksen and Bostock, 2000; Kang and Baag, 2004).

This paper focuses on *P* waves. We note that teleseismic *S* waves are usually observed at periods of several seconds and longer. Depending on the frequency of the *S* arrivals and the crustal structure, reverberations of *S* waves in the crust may also overlap with the direct *S* arrival and thus affect the travel times measured by waveform cross correlation. The

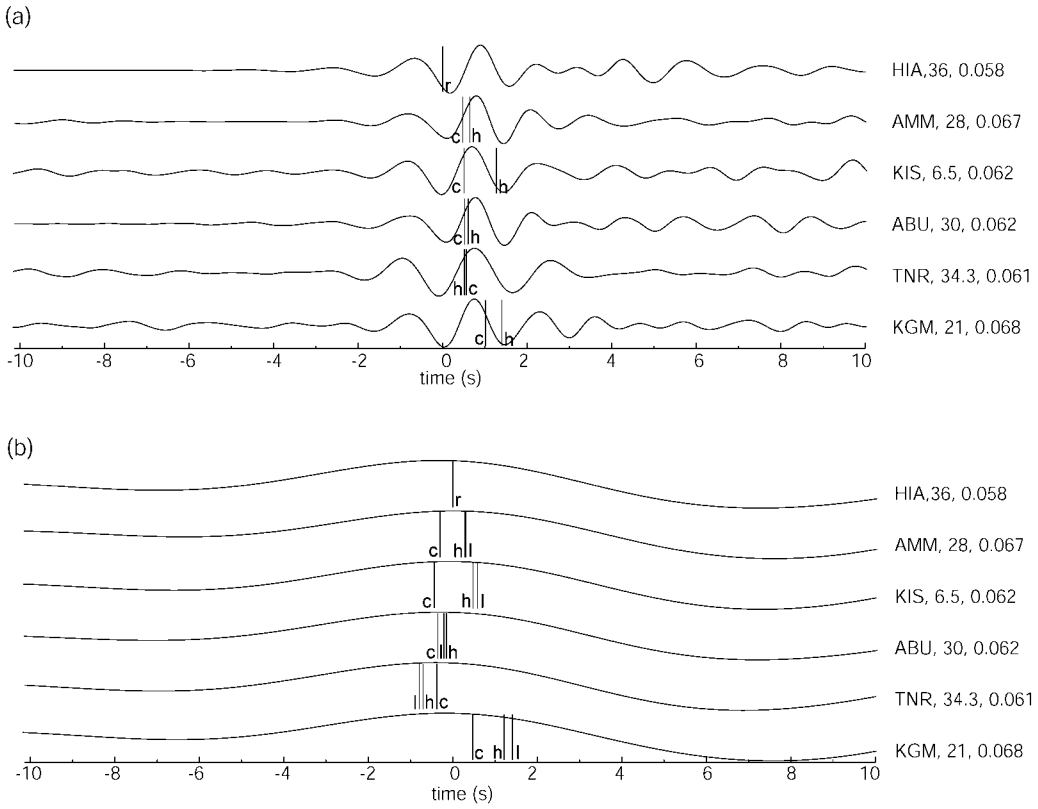

Figure 5. The filtered high- (0.5–2.0 Hz) (a) and low- (0.03–0.1 Hz) (b) frequency seismograms at six stations in the western Pacific. Seismograms are aligned according to the time shifts determined from waveform cross correlation. The vertical bars mark the time shifts (relative to the "r" bar in the first trace) calculated from the waveform cross correlation ("c"). "h" and "l" represent the adjusted time shifts after the crustal corrections estimated from the impulse response in the high- and low-frequency bands, respectively. In low-frequency seismograms (b), the time shifts with crustal corrections calculated from the high-frequency impulse response ("h") are also shown for comparison with "l". Values after station names are the thickness of the crust beneath the station in kilometers (Bassin *et al.*, 2000) and the ray parameter in seconds per kilometer The earthquake occurred at 02:45:59 on 7 September 2001, and the epicenter was at (13.16° S, 97.30° E).

frequency-dependent *S* crustal correction can be determined in the same way as outlined for *P* waves.

Conclusions

Through a series of synthetic experiments, we demonstrate that the effects of crustal structure on travel times measured by waveform cross correlation are frequency dependent. The difference in crustal correction between high- and low-frequency arrivals could reach as large as 0.65 sec for a relatively thin crust and crust with strong shallow reverberations. As a result, this frequency dependence in travel times measured by waveform cross correlation cannot be ignored in finite-frequency tomography or any tomography using low frequency or broadband body waves. The frequency-dependent crustal correction can be approximated, to first order, by cross-correlating the impulse responses of a crust model filtered in a narrow frequency band.

References

Allen, R. M., G. Nolet, W. J. Morgan, K. Vogfjord, B. H. Bergsson, P. Erlendsson, G. R. Foulger, S. Jakobsdottir, B. R. Julian, M. Pritchard, S. Ragnarsson, and R. Stefansson (2002). Imaging the mantle beneath Iceland using integrated seismological techniques. *J. Geophys. Res.* **107,** 2325, doi 10.1029/2001JB000595.

Bassin, C., G. Laske, and G. Masters (2000). The current limits of resolution for surface wave tomography in North America, *EOS Trans. AGU* **81,** F897.

Beck, S., G. Zandt, S. C. Myers, T. C. Wallace, P. G. Silver, and L. Drake (1996). Crustal-thickness variations in the central Andes, *Geology* **24,** 407–410.

Dahlen, F. A., S.-H. Hung, and G. Nolet (2000). Frechet kernels for finite frequency traveltimes. I. Theory, *Geophys. J. Int.* **141,** 157–174.

Dawson, P. B., J. R. Evan, and H. M. Iyer (1990). Teleseismic tomography of the compressional wave structure beneath the Long Valley region, *J. Geophys. Res.* **95,** 11,021–1,050.

Evans, J. R., and U. Achauer (1993). Teleseismic velocity tomography using the ACH-method: Theory and applicaiotn to continental-scale studies, in *Seismic Tomography: Theory and Practise,* K. M. Iyer and K. Hirahara (Editors), Chapman and Hall, London, 319–360.

Foulger, G. R., M. J. Pritchard, B. R. Julian, J. R. Evans, R. M. Allen, G. Nolet, W. J. Morgan, B. H. Bergsson, P. Erlendsson, S. Jakobsdottir, S. Ragnarsson, R. Stefansson, and K. Vogfjord (2001). Seismic tomography shows that upwelling beneath Iceland is confined to the upper mantle, *Geophys. J. Int.* **146,** 504–530.

Frederiksen, A. W., and M. G. Bostock (2000). Modeling teleseismic waves in dipping anisotropic structure, *Geophys. J. Int.* **141,** 401–412.

Hung, S-H, Y. Shen, and L.-Y. Chiao (2004). Imaging seismic velocity structure beneath the Iceland hot spot: a finite frequency approach, *J. Geophy. Res.* **109,** doi 10.1029/2003JB002889.

Kang, T. S., and C. E. Baag (2004). An efficient finite-difference method for simulating 3D seismic response of localized basin structures, *Bull Seism. Soc. Am.* **94,** 1690–1705, doi 10.1785/012004016.

Kennett, B. L. N. (1983). *Seismic Wave Propagation in Stratified Media,* Cambridge University Press, New York.

Kennett, B. L. N., and E. R. Engdahl (1991). Traveltimes for global earthquake location and phase identification, *Geophys. J. Int.* **105,** 429–465.

Keyser, M. J., R. R. Ritter, and M. Jordan (2002). 3D shear-wave velocity structure of the Eifel plume, Germany, *Earth Plant. Sci. Lett.* **203,** 59–82.

Kissling, E. (1993). Deep structure of the Alps—what do we really know? *Phys. Earth Planet. Interiors* **79,** 87–112.

Komatitsch, D., and J. P. Vilotte (1998). The spectral-element method: an efficient tool to simulate the seismic response of 2D and 3D, geological structures, *Bull. Seism. Soc. Am.* **88,** 368–392.

Martin, M., and J. R. R. Ritter and the CALIXTO Working Group (2005). High-resolution teleseismic body-wave tomography beneath SE Romania. I. Implications for three-dimensional versus one-dimensional crustal correction strategies with a new crustal velocity model, *Geophys. J. Int.* **162,** 448–460, doi 10.1111/j.1365-246X.2005.02661.x.

Obayashi, M., D. Suetsugu, and Y. Fukao (2004). PP-P differential traveltime measurement with crustal correction, *Geophys. J. Int.* **157,** 1152–1162.

Shen, Y., and S.-H. Hung (2004). Ridge-like upwelling in the uppermost lower mantle beneath eastern Africa from finite-frequency seismic tomography (abstract), *EOS Trans. AGU* **85,** no. 47 (Fall Meet. Suppl.), U41A-0720.

VanDecar, J. C., and R. S. Crosson (1990). Determination of teleseismic relative phase arrival times using multi-channel cross-correlation and least squares, *Bull. Seism. Soc. Am.* **80,** 150–169.

VanDeCar, J. C., D. E. James, and M. Assumpcao (1995). Seismic evidence for a fossil mantle plume beneath South America and implications for plate driving forces, *Nature* **378,** 27–31.

van der Hilst, R., and M. V. de Hoop (2005). Banana-doughnut kernels and mantle tomography, *Geophys. J. Int.* **163,** 956–961.

Waldhauser, F., R. Lippitsch, E. Kissling, and J. Ansorge (2002). High-resolution teleseismic tomography of upper-mantle structure using an *a priori* three-dimensional crustal model, *Geophys. J. Int.* **150,** 403–414.

Webb, S. C. (1998). Broadband seismology and noise under the ocean, *Rev. Geophys.* **36,** 105–142.

Wilcock, W. S. D., S. C. Webb, and I. T. Bjarnason (1999). The effect of local wind noise on seismic noise near 1 Hz at the MELT site and in Iceland, *Bull. Seism. Soc. Am.* **89,** 1543–1557.

Wolfe, C. J., I. Th. Bjarnason, J. C. VanDecar, and S. C. Solomon (1997). Seismic structure of the Iceland mantle plume, *Nature* **385,** 245–247.

Yang, T., Y. Shen, S. van de Lee, S. Solomon, and S.-H. Hung (2006). Upper mantle structure beneath the Azores hotspot from finite frequency seismic tomography, *Earth Planet. Sci. Lett.* **250,** 11–26, doi 10.1016/j.epsl.2006.07.031.

Graduate School of Oceanography
University of Rhode Island
Narragansett, Rhode Island 02882

Manuscript received 19 February 2006.